Autonomous flexible sensors for health monitoring

Huynh, Tan Phat; Haick, Hossam

Published in:
Advanced Materials

DOI:
10.1002/adma.201802337

Published: 01/01/2018

Document Version
Accepted author manuscript

Document License
Publisher rights policy

Autonomous Flexible Sensors for Health Monitoring

Tan-Phat Huynh and Hossam Haick**

Dr. T. -P. Huynh
Laboratory of Physical Chemistry, Faculty of Science and Engineering
Abo Akademi University
Porthaninkatu 3-5, FI-20500 Turku, Finland
E-mail: tan.huynh@abo.fi

Prof. H. Haick
The Department of Chemical Engineering and
The Russell Berrie Nanotechnology Institute
Technion – Israel Institute of Technology
Haifa 3200003, Israel
E-mail: hhossam@technion.ac.il

Keywords: Autonomous, flexible sensor, health, self-powered, self-healing, Internet-of-Things, self-sensing.

Abstract

This progress report aims to describe state-of-the-art solutions for the development of autonomous flexible sensors for healthcare purposes. Being, or claiming to be, “autonomous” means that the sensor is self-powered, self-sensing and self-healing. These concepts are presented separately throughout the report due to their distinctly individual research fields. Yet, in the last section they are brought together into a single platform, connecting to the “Internet of Things” (IoT).

Introduction

The term *autonomous technology* refers to devices that operate independently of any human intervention.[1] Autonomous technology can provide significant benefits, such as autonomous robotics/vehicles that can solve complex problems and security issues beyond human capabilities.[2] This report will focus on a newly emerging trend in the autonomous technology field, namely autonomous sensors for health monitoring and/or disease diagnosis. Thus, the advanced materials that can act both as sensing platforms and as autonomous elements are highly demanded.

To better understand autonomous materials and related sensors, we will briefly introduce the multiple sensory organs (skin, eyes, ear, tongue and nose) that work in an autonomous manner based on combination of sensory and brain activity. Sensing cells first utilize energy generated from nutrition to maintain their activities. Analytes or stimulants are recognized by receptors located on the surface of sensing organs. A recognition signal is then converted to an electrical signal, and transmitted to the brain for analysis.[3] Therefore, if any sensor can independently achieve a complete cycle of this process, it becomes autonomous. In order to make sensors autonomous, this report will summarize recent developments, including self-powering, self-sensing, self-healing and internet of things (IoT) materials and technologies, essential to that end. The review also points out potential applications of these sensors for health monitoring in which flexible sensors are some of the central interests of advancement.

Flexible sensors in general play a key role in early diagnosis through continuous monitoring of complex conditions (body temperature, heart rate, muscle motion, etc.) in health and disease (such as heart failure, sleep apnea, Parkinson disease, stroke, cardiovascular disease, and hypertension).[4] The cost-effective, soft, transparent, lightweight, easy-to-fabricate, biocompatible and versatile sensing systems are thus revolutionizing the sensor field. An example in this field is electronic skin (e-skin) – an imitated version of human skin – with a highly pixelated sense-of-touch that translates miniscule spatial deformation into (electronic or optical) signals,

while being durable and withstanding mechanical deformation. With additional chemical modification, e-skin could simultaneously sense different environmental parameters, such as temperature, humidity and pressure, which are crucial for health monitoring.[4a] Flexible and/or wearable sensors (e.g. smartwatch, bandage, or cloth) can then send the signals wirelessly to recording and analyzing reader devices. However, such sensors are lacking autonomy due to the drawbacks of several important integrated parts, such as batteries with finite power, and by their being breakable.

Major types of autonomous flexible sensor

Wu and Haick et al.[5] have recently reported on a seminal work on "materials and wearable devices for autonomous monitoring of physiological markers". Based on it, a new direction of autonomous technology for flexible sensors will be addressed in greater detail in this review, especially:

- self-powering using passive pump and capillary force (section 1.5);
- self-sensing sensors (section 2);
- IoT solutions for autonomous sensors (see Perspective); and
- autonomous sensors for monitoring pH, porphysome structure, and the concentrations of sodium, glucose and protein in body fluids, as mentioned throughout the review.

1. Self-powered flexible sensors

Sustainable development of green energy has provided a wide selection of different flexible energy-harvesting devices[6] from piezo-, tribo-, or thermos-electric generators to solar or radio-frequency cells, (Figure 1) and no-power-supply microfluidics[7]. Among them, the piezo-, tribo-, or thermoelectric approaches seem highly favorable, and are found in many flexible sensing systems due to their low-cost components,[8] simple and ready energy input (e.g. pressure or heat from human body) readiness, and ease of integration into flexible sensors on a single chip. Employing those types of power render self-powered sensors compact and flexible.[9]

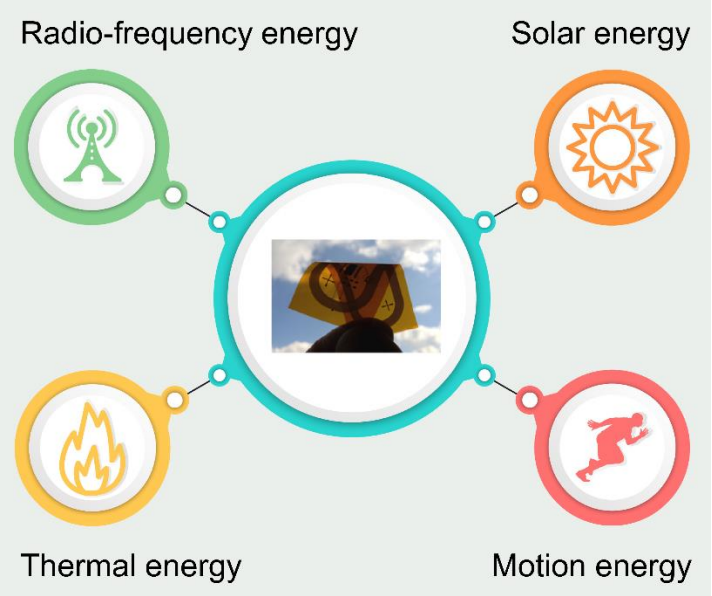

Figure 1. Energy sources for driving the self-powered sensors

1.1 Piezoelectric and triboelectric approaches

Piezoelectric and triboelectric effects are two very similar phenomena of "mechanical-electrical conversion".[10] Both piezoelectric and triboelectric materials can be operated with unlimited power sources provided by the motion/locomotion of muscles and joints, the internal movement of organs, such as the esophagus and trachea, or vibration energy from acoustic waves, thus enabling the creation of self-powered sensors.[6d, 11]

Piezoelectric effect is the ability of materials (*e.g.* quartz, silk, poly(vinylidene difluoride) PVDF, barium titanate, lead zirconate titanate) to generate an electric charge in response to applied mechanical stress (mainly compression). The simplest example of a flexible piezoelectric generator is zinc oxide (ZnO) as a thin film, the application of which in energy-harvesting is quite new, but of high potential.[12] A hybrid composite, using ZnO nanowires and piezoelectric polymers, such as polyvinylidene difluoride (PVDF), was developed using a simple and inexpensive solution-casting technique.[13] This generator delivered a maximum open-circuit voltage of 6.9 V and a short-circuit current of 0.96 μA, resulting from a uniaxial compression. An output power of 6.6 μW was used to drive a (ZnO-microwire)-based pH sensor. However, this development, based on a ZnO microwire supported on rigid glass substrate, is far from being applicable because the pH change is non-linear and of low voltage sensitivity. Surprisingly, by replacing the ZnO nanowires with Cerium(III) complex in PVDF matrix the generator produced a remarkable enhancement of the output voltage of up to ~32 V, achieved by simple repeated

human finger pressing.[14] This is believed to result from the formation of hydrogen bonds between the positive-charge Cerium complex and the induced negative-charge of PVDF, causing the formation of the β- and γ-phase PVDF – the electroactive phases. The film also photoluminesced intensely in the UV region, which makes it act as an optical transducer for flexible sensors. A piezoelectric PbZr0.52Ti0.48O3 (PZT) thin film turns flexible when fabricated on polyimine substrate by the laser-lift-off technique.[15] The authors suggested its use as a power supply for touch-screens; however, there is much more potential of this device in health monitoring, e.g. by connecting a thin-film PZT generator with a flexible chemical/biological sensor.

The triboelectric effect, on the other hand, is a type of contact electrification in which materials (e.g. human hair, wool, nylon, paper) become electrically charged after they come into frictional contact with another material. A charge can be produced triboelectrically by strain-induced stretching or bending as two materials slide over each other. This can be achieved simply using pristine organic materials, such as fluorinated ethylene propylene (FEP)[16] nanowires or polyvinyl alcohol (PVA)[17]. The conducting electrodes are either ITO-PET[16] or flexible metal foil[17]. FEP nanowires containing a high percentage of fluorine (the strongest electronegative element), is one of the most triboelectric negative materials, whereas PVA is recyclable and environmental-friendly. More interesting, electrical generation happens when Ag nanowires (AgNWs) rub against each other in a copolymer matrix of poly(3,4-ethylenedioxythiophene)-poly(styrenesulfonate)/polyurethane (PEDOT-PSS/PU).[18] The PEDOT-PSS/PU layer is used to conduct charge generated from the AgNWs to the sensor. The thin film of AgNW/PEDOT-PSS/PU is attached to polydimethylsiloxane (PDMS) and poly(ether sulfone) (PES), resulting in high sensitivity, stretchability and optical transparency (Figure 2a1),. The energy is stored in a supercapacitor, which provides power storage to operate the strain sensor (Figure 2a), and this provides a self-powered monitoring system for movement of the tracheal region of the neck. When placed on this region (Figure $2b_1$), the sensor can recognize a wide range of strains on the skin (Figure $2b_{2\text{-}6}$), which gives it the prospect of being developed into a transdermal patch for body-part motion. In another example, with graphene – a material with abilities of storing electric charges for a period of time and providing a large surface area for contact electrification/triboelectric effect[19] – in the polymer PEDOT-PSS based composite, the nanogenerator had a current density as high as 2.4 μA/cm^2 and 12 μW in power.[20] Furthermore, the composite electrode had high physical and electrical durability for 10,000 bending cycles, and the production of the generator could be scaled up to an area of 100 cm^2.

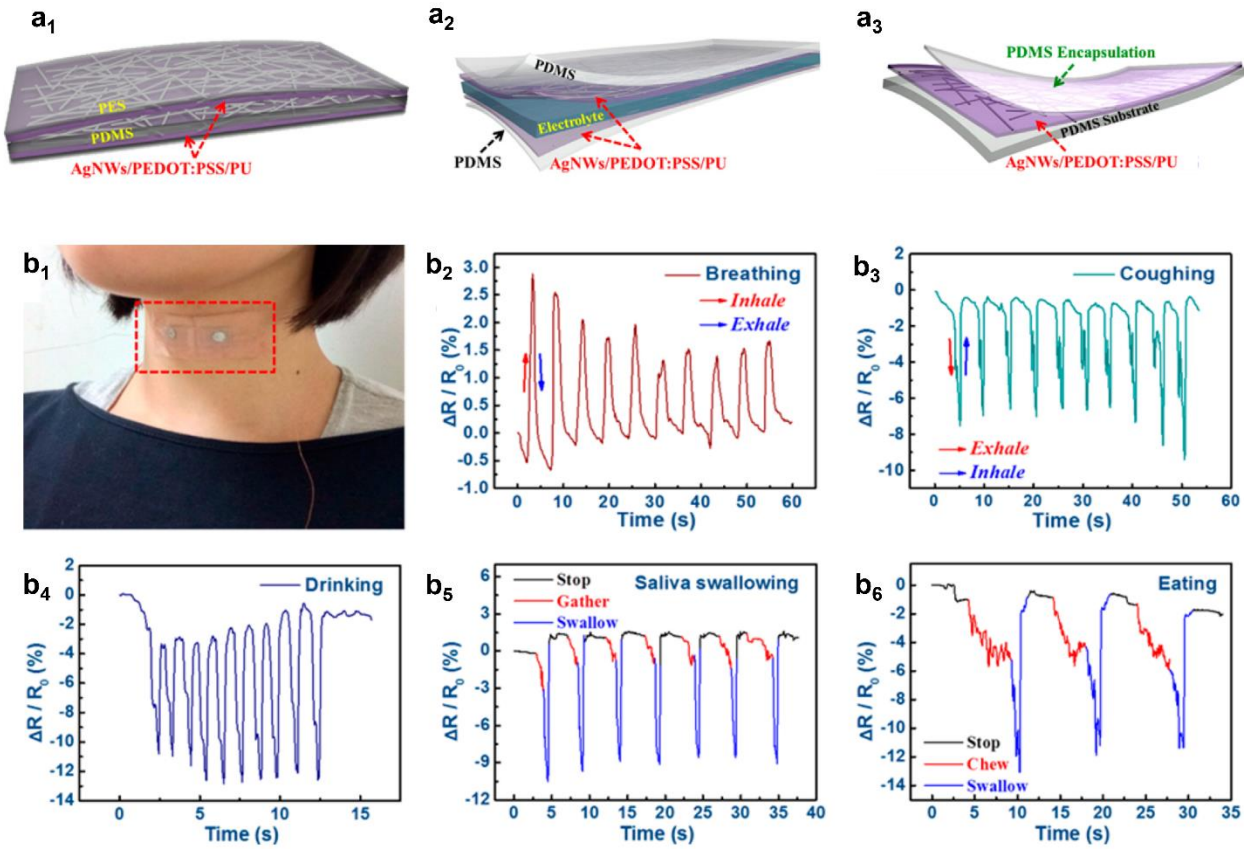

Figure 2. (a) Schematic architecture of a self-powered strain sensor including (a_1) triboelectric nanogenerator, (a_2) supercapacitor, and (a_3) strain sensing unit. (b_1) Sensor located at the tracheal region of neck for monitoring resistance change ($\Delta R/R_0$) of the nanocomposite strain sensor versus time during (b_2) breathing, (b_3) coughing, (b_4) drinking, (b_5) saliva swallowing, and (b_6) eating, respectively. (Reproduced with permission from ref. [18]; copyright 2015 ACS Publications)

Instead of a capacitor, a flexible lithium-ion battery belt was used to store charge from a triboelectric-based textile cloth.[21] The Ni films, coated on polyester fabrics, were used both as electrodes in the triboelectric-based cloth and current collectors in the belt. Contact electrification, i.e. electron transfer from the tribopositive Ni film to the tribonegative parylene film occurs when they are brought into close contact. The triboelectric-based cloth could convert body movement, e.g. in particular, motion in the area around stomach, into electricity. The battery belt then powered a commercial heartbeat sensor (ATECH@) which is capable of remote communication with a smart phone through Bluetooth. The belt showed decent electrochemical performance even after being severely folded 30 times at 180°.

Interestingly, a triboelectric generator can be operated without charge storage by using streaming potential/current phenomenon[22] from which K^+ ions are formed triboelectrically next to a negative-charged surface of porous PDMS. Flow of K^+ ions driven by syringe pump generates electrical energy to power a ZnO-nanowire pH sensor. However, it is challenging to generate charges for solution of low-concentration or no electrolyte in which the layer of cations cannot be formed.

1.2 Thermal approaches

The thermoelectric effect, the conversion of thermal energy into electricity, is based on the Seebeck effect, where an open-circuit voltage ΔV develops between thermocouples (combination of 2 different materials).[23] Thermoelectric materials can transform thermal energy from a temperature gradient of different heat sources, e.g. from body or indoor/outdoor heat, into electricity.[24] A thermoelectric generator therefore has the advantage of having no moving mechanical parts (like piezoelectric or triboelectric generator), making it useful for integration on flexible modules for health monitoring applications.

By far the most widely used thermoelectric materials are p-Sb_2Te_3 and n-Bi_2Te_3 because of their high thermoelectric efficiency at around room temperature.[25] According to one proof-of-concept prototype, an array of 100 thin film thermocouples of p-Sb_2Te_3 and n-Bi_2Te_3 was sputtered on Kapton polyimide foil. With an output of ΔV of ~160 mV and electrical power of 4.18 nW, this flexible generator only fits applications of very-low power consumption. Moreover, several tests are needed regarding its biocompatibility and the stability of the thermal electric layer under deformation.

While not as efficient as the above inorganic thermoelectric materials, PEDOT:PSS coating has been used as power supply on top of a flexible microstructure sensor for temperature and pressure (Figure 3a).[26] The generator provided a typically lower than 1 mV output voltage. Advantageously, the pressure sensing performance of the sensor was independent of the biased voltage over a wide range (from 30 mV to 1.5V), allowing the effective transduction of temperature and pressure stimuli into 2 distinct electrical signals. This permitted the instantaneous sensing of temperature and pressure, with an accurate temperature resolution of <0.1 K and a high-pressure-sensing sensitivity of up to 28.9 kPa^{-1} (Figure 3b). The excellent sensing properties of these sensors, together with their unique advantages of low cost and large-area fabrication, make these materials worth considering for applications in e-skin and health-monitoring elements.

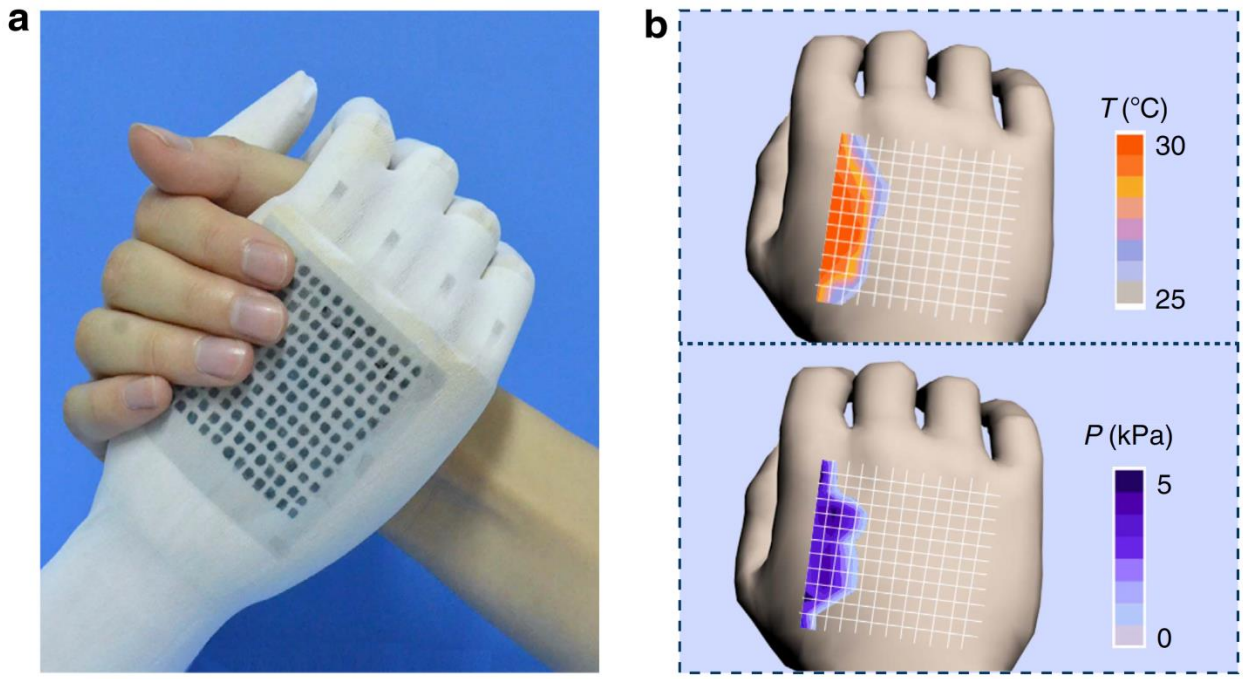

Figure 3. Demonstration of a thermoelectric-powered device. (a) Photograph of a prosthetic hand arm-wrestling with an adult woman. (b) Temperature and pressure mapping profiles of pixel signals on the back of the prosthetic hand. (Reproduced with permission from ref. [26]; copyright 2015 SpringerNature).

1.3 Solar approaches

Light harvesters are also being considered as power supplies for flexible sensors due to frequent exposure of wearable devices to redundant sunlight. Solar harvesting technology has been growing fast to provide a wide range of choice from inorganic to organic materials and, more important, from rigid to flexible substrates.[6c, 27] For instance, a self-powered wearable wireless sensor node for biometric monitoring has been proposed.[28] The design included an ultralow power circuit printed on a flexible substrate. This flexible circuit helps to transfer near maximum electrical power, which is converted from solar energy using an amorphous silicon photovoltaic panel to be stored in a supercapacitor. For multiparametric sensing, a novel wearable smartwatch with epidermal temperature sensors powered by silicon solar modules mounted on the band wrist has been developed.[29] The sensing device includes an array of 16 sensors on a flexible Kapton substrate to monitor pH in sweat with low -power consumption of 2 mW. The sensor's technique leads to ambitious plans for the detection of different diseases (for example, kidney and diabetes).[30] Compared to tribo- or piezo-electric or thermal generator, solar cells consist of many

parts, making their structure more complex, presenting a challenge in their assembling into flexible sensors.

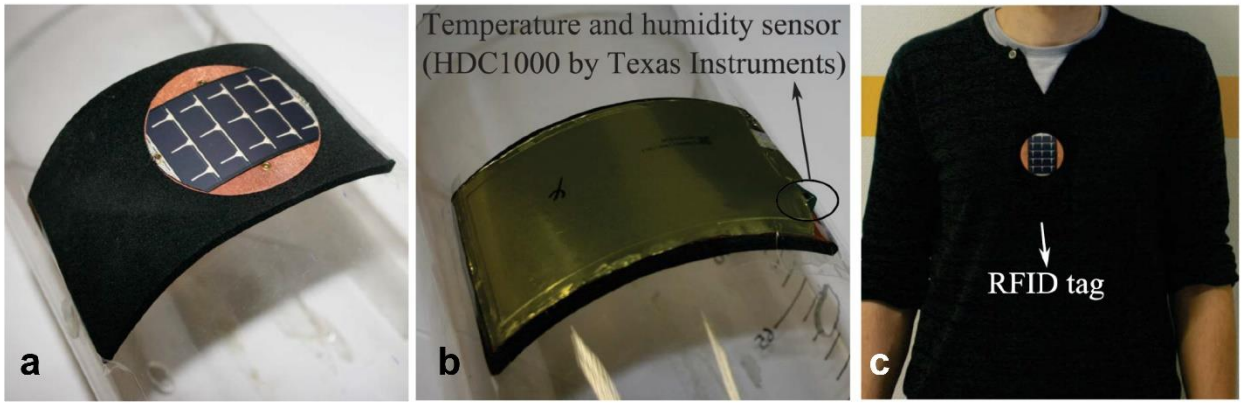

Figure 4. Prototype of a flexible complex including the RFID tag with integrated light-harvester and battery (a) top view, (b) bottom view, and (c) on-body deployment. (Reproduced with permission from ref. [31]; copyright 2016 IEEE*Xplore*).

A compact design was achieved by integration of a hydrogenated-amorphous-silicon solar cell on the top of the wearable active radio frequency identification (RFID) tag, which operated at 2.45 GHz (Figure 4).[31] A flexible battery is an energy storage for night-time use. The textile antenna's functionality is exploited by a neat all-in-one comfortable design for stable radiation performance. The working range of the RFID tag sensor is up to 23 m under real-life conditions, and the RFID platform only consumes 168.3 μW in every 60 s while maximum power of the solar cell is up to 50 mW under standardized illumination of 100 mW/cm^2. The tag features flexible interfacing low-power humidity and temperature sensors via the I^{2}C bus as a proof-of-concept. The design is highly convenient for tracking health conditions of patients in hospital.

1.4 Radio-frequency approaches

RF electronics and RFID tag-based sensors also play an important role in self-powered sensors.[32] Unlike the active RFID tag mentioned above, which requires connection with power supply, e.g. a solar cell to power it using radio frequency, an passive RFID tag can power itself from the inductance of the loop antenna by extracting power from the active RF source. This lets the device operate anywhere and last almost forever. Moreover, the recent RFID tags are thin and flexible making them embedded easily in human body towards health monitoring.[33]

The incoming radio signal, either in the High Frequency (HF, 13.56 MHz) or Ultra High Frequency (UHF, 400 MHz) band, has proven adequate to power the adaptive threshold rectifier.

The HF band is for patch sensors, whereas the UHF band is supported for implantable sensors.[34] The sensor consumes 12 µW to implement an electrocardiogram analog front-end, and an Analog-to-Digital Converter (ADC). A pair of planar-fashionable circuit board (P-FCB) electrodes is capacitively coupled to the instrumentation amplifier input. Due to the low efficiency of P-FCB inductors, the amount of generated power is very limited, so the overall power budget of the sensor is designed to stay below 20 µW. Even though the bandage is wearable, it covers the whole chest, making it inflexible for application.

Neat design for flexible RFID tags therefore open many applications in healthcare such as sensing of moisture,[35] volatile organic compounds (VOCs),[36] and hydrogen gas[37]. Size of all these RFID-tag based sensors are not larger than a human palm. UHF band (between 800 and 1000 MHz) were used to power the passive RFID tags. The tag can be used either unmodified for moisture sensing due to degradation of the tag performance[35] or modified with functional materials, e.g. carboxyl-functionalized polypyrrole nanoparticles and Pt-decorated reduced graphene oxide (rGO), for selective sensing of VOCs and hydrogen gas[36-37]. Expectedly modified sensors manifested lower limits of detection (LOD), i.e. ppb range for VOCs and 1 ppm for hydrogen. Moreover, these sensors maintained their sensing performance as they had been deformed by bending and twisting, making them highly potential for point-of-care testing.

1.5 Other self-powered devices

Self-power can be achieved electrochemically by fabricating an electrochemical cell from metal–GO junction on a flexible paper substrate.[38] The power generation mechanism is attributed to delivery of trace amount of electrolytes from human fingers to the junction; when touched it triggers electrochemical reaction. The platform was utilized as humidity and tactile sensor. However, there is a challenge in this work because moisture could also trigger an electrochemical reaction, which makes power generation from it uncontrollable in high humidity conditions.

All examples of self-powered flexible sensors discussed so far rely on energy sources and harvesters.[5] Powerless passive pump (absorbent)[7a] and capillary force[7b, 7c, 39] supplying pumping action for an autonomous microfluidic chip has emerged as alternatives. These methods give a much simpler design for flexible sensors compared to electric generators mentioned above, due to elimination of a power supply and the need for storage. When the system (Figure 5a) is in its dry state, the rate of passive fluid pumping at a few µL min^{-1} through the channel is due to the natural absorption of the cotton thread placed into the channel. The sensing unit installed is Nylon Lycra® textile with a bromocresol purple (BCP) pH sensitive dye. The color variation generated by the pH change was recorded using the SMD LED-light photo sensor. The device exhibited

linear response in a range of 6 to 9 pH value leading to trial test on measuring pH of human sweat.[7a] A paper-based flow system (Figure 5b) drives flow by capillary forces developing in the narrow gap between 2 parallel surfaces separated by a spacer. The top surface is hydrophobic, whereas the bottom consists of a hydrophilic pathway surround by a hydrophobic paper substrate. As a result, the liquid flows on the hydrophilic path in the gap without spreading onto the hydrophobic regions. The sensor can detect excess bovine serum albumin (BSA) protein or glucose in urine through the color change of indicators (tetrabromophenol blue and horseradish peroxidase/glucose oxidase, respectively) located at the reaction zones. LOD for BSA and glucose are as low as 7.5 µM and 5 mM, respectively.[7c] In a more advanced development, Rogers et. al. demonstrated that capillary-driven microfluidic devices integrated colorimetric indicators (e.g. cobalt or iron complexed dyes[39a, 39c] and organic dyes[39b]) are highly biocompatible, flexible, stretchable, and watertight. The color change from these indicators pictured and analyzed by smartphone were used either to detect UV irradiation[39b] or to sense a wide range of biomarkers in sweat such as chloride and hydronium ions, glucose, and lactate[39a, 39c]. Additionally, these sensors were tested practically on different parts of human skin making them become commercialized products for health monitoring.

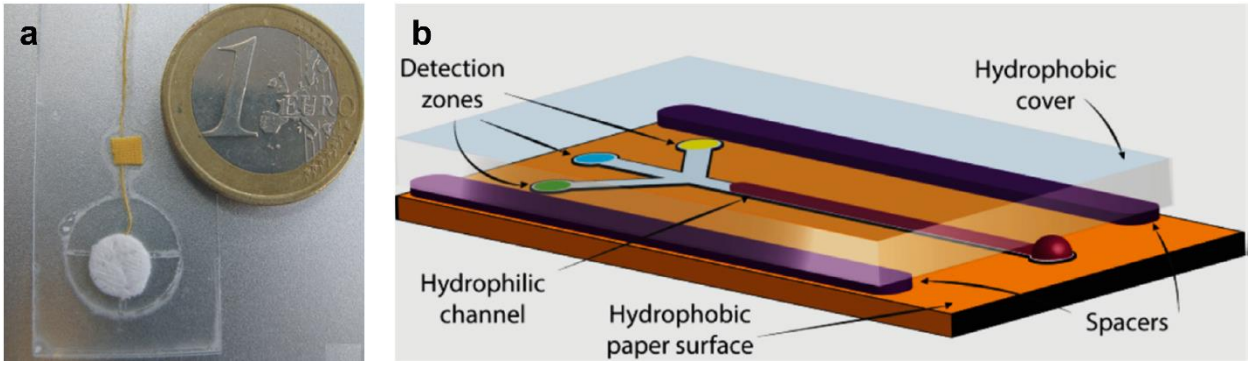

Figure 5. (a) A passive-pump self-powered micro-fluidic chip (reproduced with permission from ref. [7a]; copyright 2012 Elsevier). (b) A paper-based capillary-driven microfluidic system. (reproduced with permission from ref. [7c]; copyright 2016 ACS Publications).

2. Self-sensing flexible sensors

Self-sensing is the method of using smart materials as both recognition unit and transducer to actuate and sense concurrently. The materials must be highly sensitive to deformation or micro- or nano-defects. Self-sensing was observed through a intact/disrupted form of porphysome nanovesicles (spherical nanovesicles formed by self-assembled porphyrin and lipid-bilayers) where the change of their structural state is spread by its fluorescence intensity. [40] Self-sensing

of porphysome nanovesicles are used in the treatment of tumors, where the treatment time is indicated by the greatest concentration of structurally intact porphysomes accumulated in the tumor. In the field of mechanical/civil engineering self-sensing sensors are capable of directly measuring local deformations of themselves, which is termed “structural health monitoring” (SHM).[41] In a sensing application, it is important to distinguish between self-sensing and external-sensing because the latter requires external sensing detectors to capture the defect or failure of sensors.[42] Additionally, self-sensing devices are different from strain/pressure sensors, where stimulants from the surrounding environment deform the sensors.

Materials for self-sensing sensors vary from fibers/fabrics to synthetic polymers/elastomers.[43] The fabrics are composed of uniform, flexible, and semitransparent graphene and can be assembled into piezoresistors for flexible touch sensing.[43a] Similarly, a graphite self-sensing film has been obtained by casting graphite-dispersed PU solution onto a glass-fiber reinforced plastic substrate.[43b] In another example, the formation of conducting polymer nanocomposite piezoresistive sensors at the fiber/matrix interface with large, stable and reliable electrical responses has been described.[43d] The self-sensing mechanism of these sensors is based on changes in their piezoresistivity under internal strains occurring inside the composite structures.

The most potentially suitable method for self-sensing application is an ultralight (density 5.8 mg cm^{-3}) magnetic elastomer, Fe_3O_4/graphene, where its electrical resistance is deformation-dependent.[43e] The 3D network of Fe_3O_4/graphene aerogel is assembled by restoring the conjugation of sp^2 regions and π-π stacking interactions between the 2D graphene sheets. The aerogels have up to 52% reversible magnetic field-induced strain and strain-dependent electrical resistance that can be used to self-sense the degree of structural inflammation of the material. Self-sensing was also found in the form of an ultra-thin and flexible array platform (Figure 6), where failure of the complete system was due to the failure of an individual sensor. The array self-sensed its actual shape by analyzing signals from 6×6 piezoelectric sensors printed on a polyimine substrate.[43f, 43g] The sensor array had the potential for surface reconstruction that correlated with the deformation geometry of the array. Such surface reconstruction with this detection potential could provide diagnostic information on, e.g., pneumothorax disease.

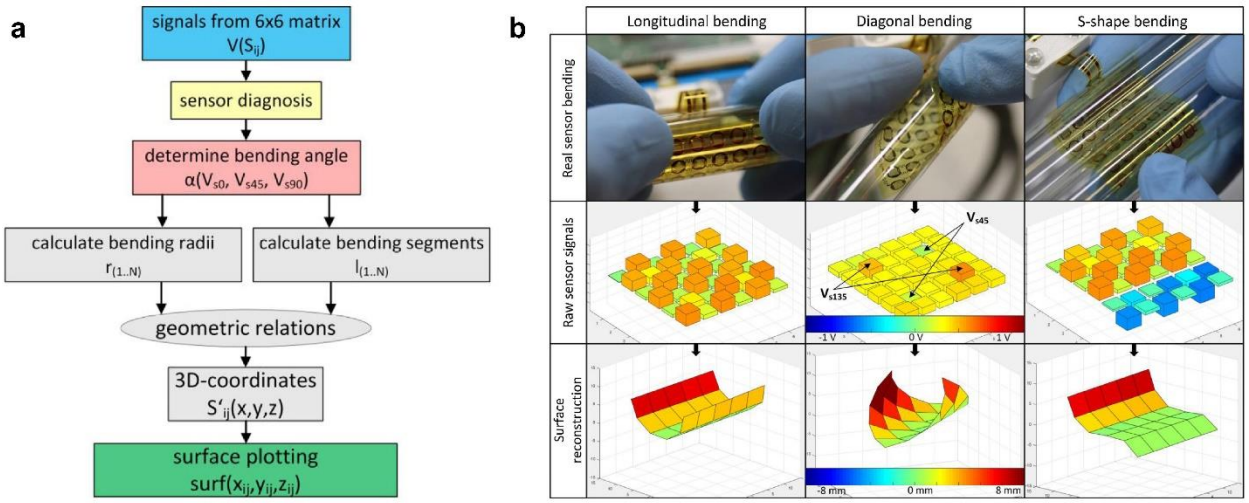

Figure 6. (a) Flow chart of the surface reconstruction process; and (b) surface reconstruction results when bending the sensor array in 3 different modes. (Reproduced with permission from ref. [43g]; copyright 2017 Elsevier).

3. Self-healing flexible sensors

To complete the review of fully autonomous sensors, a flexible sensor can not only detect its structural problems, i.e. self-sensing, but also fix them. Thus, a new aspect of smart sensors is in development, namely self-healing technology, where certain materials can repair themselves.[44] Self-healing must occur at ambient conditions without the need for any trigger or external stimulus. This report will discuss both intrinsic and extrinsic self-healing polymers. Intrinsic self-healing is based on molecular interactions (e.g., hydrogen bonding, π-π stacking, and metal-ligand coordination)[45], whereas extrinsic self-healing polymers are dependent on the release of monomers and catalysts packed in capsules or vessels that become dispersed in an otherwise non-healing polymer.[46] Although extrinsic self-healing materials are more efficient in recovering larger scale damage compared to intrinsic materials, they are, however, less suitable for flexible thin devices because they are not easily fabricated, and their integration into fully functional applications - especially in health monitoring applications - is complicated. The intrinsic self-healing polymers are more advantegous due to their ability to reversibly heal themselves multiple times due to functionalization of polymer with different self-healing groups[45, 47]. Another benefit of using an intrinsic polymer is its fast healing due to the absence of diffusion and polymerization control steps, which are crucial for the application in wearable devices, where signal interruption due to damage has to be avoided or repair must occur as quickly as possible. Moreover, due to the demand for extending their potential uses, intrinsic self-healing polymers have been modified by various means to achieve high flexibility, fast self-healing, biocompatibility, as also to obtain

many physical (e.g. electrical, electronic, and thermal) and chemical (e.g. electrochemical and photochemical) properties.[48] Therefore, the development of self-healing properties for electrical or electrochemical sensing devices constitutes a major challenge. A partially or fully self-healing sensor would give much more reliable and stable data.[49]

Bao et al.[50] provided the first example of a self-healing conductive composite using a urea-based self-healing polymer and nickel microparticles (μNi) as filler (Figure 7a). A thin native oxide layer covered μNi enhanced hydrogen bonding within a μNi and polymer network, in which the volume percentage of the μNi could be up to 31%. Conductivity at 40 S cm^{-1} can be reached by adding +15% volume fraction of the μNi and composite, which have both electrical and mechanical self-healing abilities at room temperature. The composite is highly responsive to the healing process, with 90% of its original conductivity being recovered within 15 s at room temperature. The use of this self-healing conductor as e-skin has been successfully demonstrated.

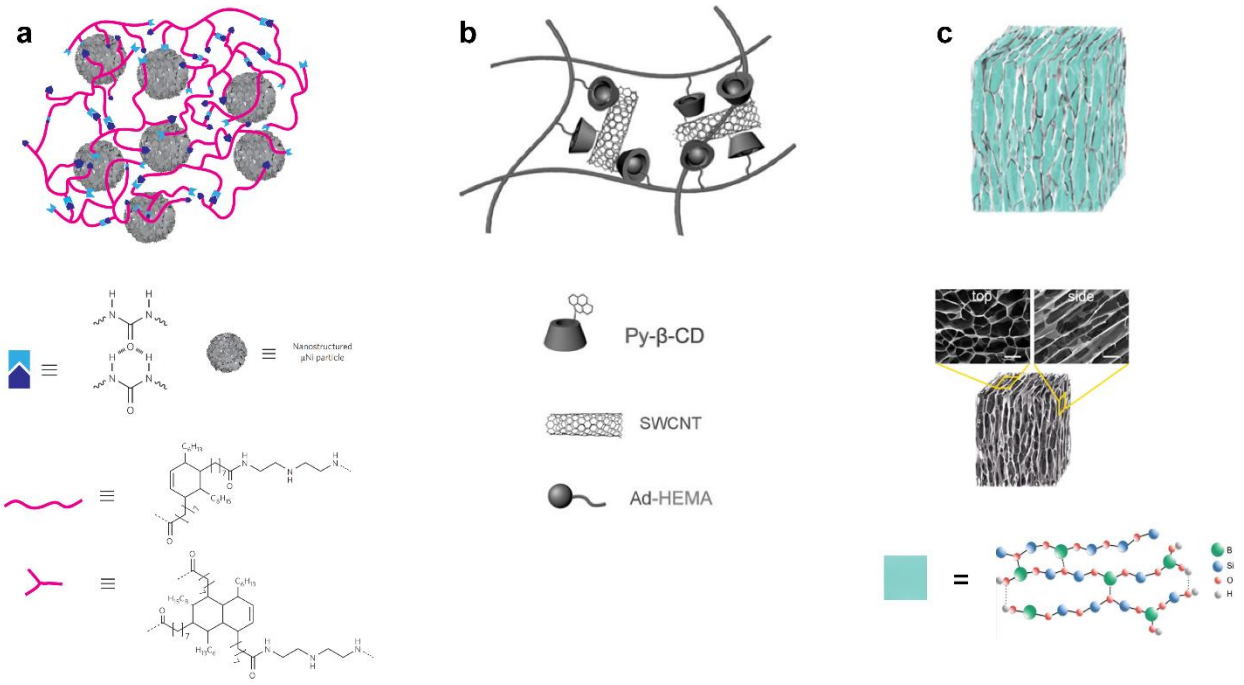

Figure 7. (a) Self-healing conductor based on a composite of self-healing branched polymers with urea groups at the end and nickel microparticles. (Reproduced with permission from ref. [50]; copyright 2012 Nature Publishing Group). **(b)** Schematic preparation of conductive self-healing composite, PHEMA-CNT-(β-CD), using inclusion chemistry between β-CD and HEMA (Reproduced with permission from ref. [51]; copyright 2015 WILEY-VCH). (**c)** rGO/PBS networks contain microscopic channels (PBS) separated by thin walls (rGO), which are packed to form a

honeycomb cross-section with residual porosity in the composite of <1%. (Reproduced with permission from ref. [52]; copyright 2015 WILEY-VCH).

Carbon-based materials, including carbon nanotube (CNT) and reduced graphene oxide (rGO), are favorite among conductive materials that chemists are trying to develop due to their unique properties, such as high electron conductivity,[53] well-developed routes of functionalization,[54] and low percolation threshold of composites.[52, 55] Unsurprisingly, the self-healing polymer could also incorporate CNT to form a composite for humidity and touch sensing.[51, 56] The self-healing conductive composites can be formed through either inclusion (host-guest) chemistry of poly(2-hydroxyethyl methacrylate) (PHEMA) and β-cyclodextrin (β-CD) followed by polymerization (Figure 7b),[51] or muscle-inspired coordination chemistry between PVA and sodium borate[56]. Inclusion (or host-guest) chemistry is a complex formation between a cavity of the "host" compound and a molecule of the "guest" compound. Even though the PHEMA-β-CD composite has a higher conductivity (~60 S cm^{-1}) than the above mentioned self-healing composites and a wide linear range of response to humidity (from 30-90%), its percolation threshold (7-11 *wt*%) is quite high, leading to an increase in a glass transition temperature of the composite. As a result, the material becomes stiffer, making self-healing inefficient because of restricted movement of the polymer chains.

Networks of rGO were infiltrated with a solution of polydimethylsiloxane (PDMS) and boron oxide nanoparticles by vacuum casting. The rGO/polyborosiloxane (rGO/PBS) composite was formed by in-situ cross-linking at 200°C.[57] PBS is a supramolecular polymer of an intrinsic self-healing character due to its dynamic dative bonds between boron and oxygen in the Si-O groups and hydrogen bonds between residual -OH groups at the end of some unreacted polymer chains. The resulting composites comprise an rGO continuous network confining PBS (Figure 7c). The first highlight of this hybrid material is its very high electron conductivity of ~8×10^3 S cm^{-1}, probably the highest conductive self-healing composite ever developed because of its high density and the uniform honeycomb structure of rGO. Second is a low percolation threshold (0.5 *wt*%) of rGO used in this composite, which is difficult to achieve by normal dispersion techniques. Therefore, self-healing of this polymer is efficient with almost 100% recovery, and the composite film is manifested as a sensitive flexion sensor. In contrast, another self-healing composite prepared by mixing and grinding graphite and polyethylenimine (PEI) creates several challenges[58] - a very high percolation threshold (65 *wt*% graphite) and lower conductivity (1.98 S cm^{-1}) compared to the rGO/PBS composite.

A multifunctional self-healing sensing device has been reported[12b] (Figure 8). Its substrate and electrodes were made from self-healing materials, the main self-healing component being a newly synthesized PU derivative. Its self-healing mechanism is based on reformation of hydrogen and disulfide bonds between polymer chains at 2 sides of the cut (Figure 8b). Healing time and efficiency of this PU depends on the density of hydrogen bonds, created by the urea groups of PU, and on disulfide bonds and the flexibility of the polymer chains. The polymer has been used as a self-healing substrate; its composite with silver particles (of micron size) works as a self-healing electrode of a chemiresistor. The electrode has to pass electrical current through the sensing layer, which is made of organic-capped gold nanoparticles (AuNP) that have an electrical resistance in the range of hundreds of kΩ to a few MΩ. The resistance of this layer varies with changes in the immediate environment (pressure, temperature, presence of gaseous compounds). So far, the organic-capped AuNP layer does not have intrinsic self-healing properties; however, its healing process is achieved by an "induced" process, viz. due to the self-healing process of the polymeric substrate laying beneath it. To demonstrate the device's functions, the self-healing chemiresistor was exposed to different environments (Figure 8c), pressure or strain (Figure 8c_{1-2}), and VOCs (Figure 8c_3)[12b, 59] known to have an important role as a "primary prevention" strategy of disease(s) through breath or skin sampling.[59-60] The sensors showed ppb-range LOD for most of VOCs and negligible difference was observed in LOD and sensitivity of the sensors before and after cutting. Similar results were also seen in pressure or strain sensing.

"Induced" self-healing is also performed on conductive CNTs[61] or CNT-polyaniline (CNT-PANI) films.[62] In the first example, the aligned wire-based CNTs between the 2 cross-sections are reconnected by Van der Waal's forces[63] during the self-healing process of the fiber. The fiber can be made from a composite of carboxyl cellulose nanocrystals and chitosan-decorated epoxy natural rubber latex,[61b] which creates multiple hydrogen bonds probed by band changes of the functional groups in FTIR spectra. A strong adhesive force is produced between aligned CNT arrays and different substrates by Van der Waal interactions. Although these forces are weak, their collective effect within a density range of 10^{10}-10^{11} cm^{-2} produces a strong adhesive force. In case of the CNT-PANI film coated the self-healing PDMS, this was used as a simple and efficient chemiresistor for NH_3 gas, for which LOD is as low as 5 ppm.[62] Preparation of the self-healing PDMS substrate is simply by mixing commercial Sylgard 184 with 1,3,5-triformylbenzene to form a reversible covalent imine bond.[64] Additionally, this is one of few self-healing polymers that has high transparency (~80%) and stretchability (~700%).

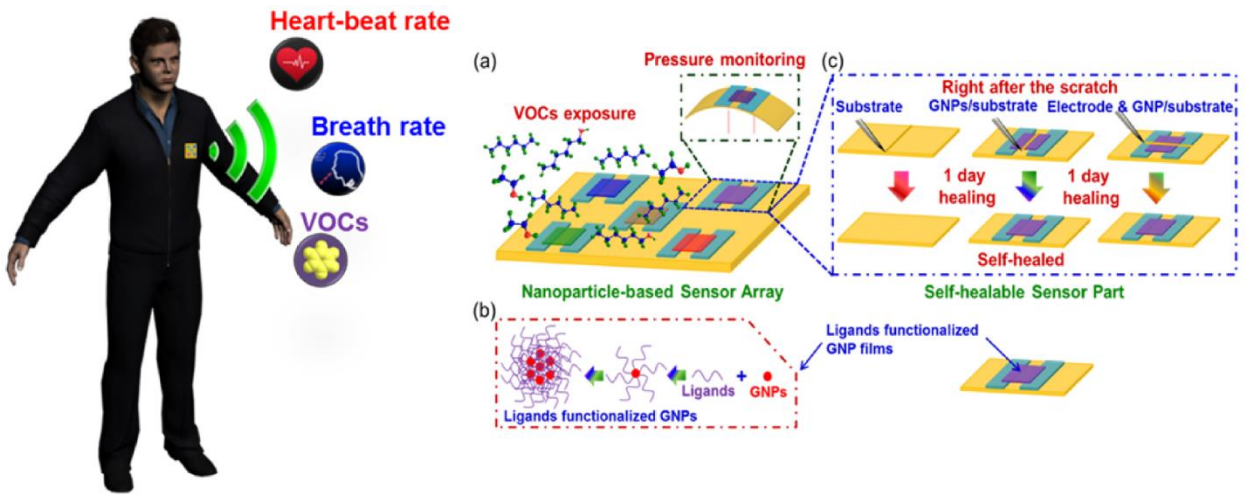

Figure 8. Illustration of the self-healable AuNP-based sensor and the overall experimental strategy. (a) Schematics of sensor array consisting of 5 self-healable sensors, each of which is based on polymer substrate, sh-μAg-PU electrodes and a molecularly-functionalized GNP film. (b) Molecular structures used for the functionalization of the GNPs (3-ethoxythiophenol, benzylmercaptan, tert-dodecanethiol, hexanethiol and decanethiol). (c) Demonstration of the 3 different cutting/scratch modes of the self-healing sensor.[59] (Reproduced with permission from ref.[59]; copyright 2016 ACS Publications).

A film of capsule-based self-healing ink as working electrodes has been used in polyethylene terephthalate (PET)-based flexible electrochemical sensors for voltametric determination of sodium, using 10 mM ferricyanide in 1 M phosphate buffer (pH 7.0) as the redox probe.[65] After mechanical damage, the capsules in the polymer film are ruptured, releasing the hexyl-acetate healing agent in the crack. This agent dissolves the acrylic binder locally, leading to redistribution of the filler particles and restoration of the conductive pathway. Even though this approach has been successful in producing self-healing conductive ink,[66] its main drawback, like other capsule-based self-healing materials, is being a single-time self-healer, i.e. if the cut reappears in the same location, healing will be inefficient or fail. Moreover, this technique cannot be applied under flow conditions because the carrier solution dilutes the healing agents.

Perspectives

The self-powered, self-sensing and self-healing flexible sensors for health monitoring have been presented separately in this report. This is how the current technologies contribute to the autonomy of sensors. Architectural design towards more comfortable and convenient sensors is

one thing, but more important is how to unify them into one complex structure because health data are mostly being detected from complex data. Although the challenge remains, any benefits deduced from "single" autonomous sensors are much greater, such as the minimum of electrical components/connections, auto-administration, low-cost maintenance and remarkable persistence. To the best of our knowledge, the "single" autonomous sensor has not so far been achieved; nevertheless, the idea is applicable through following aspects

- Synergy of two or more "self"-abilities in one device, for example, inserting self-healing into energy harvester is state-of-the-art.[67] The research outcome is freshly developed self-healing triboelectric generators.[68] The first significant improvement is replacement of the metallic electrodes of the generator by slime-based ionic conductors, which is self-healable.[68a] Self-healing of the slime layer starts from multiple hydrogen bonds formed between PVA and borax. The latter development is more complete where the generator has been made of self-healing PDMS-PU copolymers and self-healing is assisted by magnetic force.[68b] Recently, a combination of two (thermoelectric and triboelectric) generators in one wearable self-powered device[69] is a wise development because one generator will be a backup for another in case of lacking energy sources. The research demonstrated the conversion of water vapors and wind up to 184.32 μW and 4.74 mW, respectively using this hybrid generator.
- Autonomous control, including self-powered, -sensing, -healing, can be correlated and integrated into a network architecture or platform using the Internet of Things (IoT). Wireless transmission between flexible sensors and hosting devices/servers is considered the key technology to be the development for enabling the use of IoT.[70] Below is a direct continuation of our discussion on the potential use of IoT in autonomous sensors.
  The *"Things"* we would like to mention in this respect are flexible sensors for healthcare.

Assuming that each person possesses hundreds of sensors,[71] the total number of sensors in a family/city/country would grow exponentially. Not only huge in numbers, these sensors are different in size, shape and rigidity. What way is therefore suitable to connect all the sensors and analyze their data? An excellent solution is the Internet of things (IoT): "A global infrastructure for the information society, enabling advanced services by interconnecting (physical and virtual) things based on existing and evolving interoperable information and communication technologies."[72]. Thus, the core idea of IoT is creating a new concept of connecting anyone, anything, anytime, anyplace, any service and any network.

As a proof-of-concept of IoT applications, a wearable microfluidics sensor, using a substrate-integrated waveguide (SIW) slot waveguide antenna for real-time detecting changes in relative-permittivity (ε_r) of fluids (herein air, water and ethanol) with a sensitivity of 1.7 MHz/ε_r value, has been described.[73] The sensing platform is fabricated with a 3D printing technique, which enables fast-prototyping-customized device for monitoring body fluids in the near future. The 3D shaped SIW transmission lines proved to be highly flexible and potentially amenable for producing useful sensors.

The near-field communication protocol also provides wireless devices with accessibility to Wi-Fi and ZigBee-based IoT sensing systems.[74] Powered by a Bluetooth module, flexible sensors, using vertically-aligned CNTs for strain sensing, provide wireless heart pulse monitoring.[74a] The high gauge factor (up to 367 for 12.5-μm-height CNTs) of the sensor is obtained by packaging CNTs, which enhances the contact area between the CNTs. The data generated from the wireless sensor are quickly uploaded and analyzed by cloud computing. The later approach with ZigBee relies on connecting a high-performance electronic circuit board to a fully degradable sensor for the monitoring of intracranial pressure.[74b] Notably, the degradable polymer herein is Ecoflex (a commercialized product of BASF), and is used as the flexible substrate and wire coating. It degrades to the basic monomers 1.4-butanediol, adipic acid and terephthalic acid and eventually to carbon dioxide, water and biomass within few weeks when metabolized in the soil or compost under standard conditions.[75] The stability in output signal of the sensor favorably matches that of a conventional thermistor, with ~0.2 K resolution. This temperature sensor seems very promising for applications in hard-to-reach environments and post-surgery healing processes.

Acknowledgments

TPH thanks the starting fund from AAU's Research Profiling (Grant No. 301843). The authors thank Dr. W. Wu and Dr. Meital Segev-Bar for fruitful discussions.

References

[1] C. Mitcham, *Encyclopedia of Science, Technology, and Ethics*, Macmillan Reference USA, Farmington, Hills, MI, **2005**.

[2] a) M. T. Penella, M. Gasulla, in *IEEE Instrumentation & Measurement Technology Conference IMTC 2007*, Warsaw, **2007**, pp. 1-5; b) D. C. Slaughter, D. K. Giles, D. Downey, *Comput. Electron.*

Agric. **2008**, *61*, 63-78; c) G. P. Moustris, S. C. Hiridis, K. M. Deliparaschos, K. M. Konstantinidis, *Int. J. Med. Rob. Comput. Assisted Surg.* **2011**, *7*, 375-392.

[3] K. S. Saladin, *Anatomy and Physiology: The Unity of Form and Function*, 3rd ed., Mc Graw-Hill, **2004**.

[4] a) S. C. Mukhopadhyay, *IEEE Sens. J.* **2015**, *15*, 1321-1330; b) C. Perret-Guillaume, L. Joly, A. Benetos, *Prog. Cardiovasc. Dis.* **2009**, *52*, 6-10.

[5] W. Wu, H. Haick, *Adv. Mater.* **2018**, 1705024.

[6] a) Y. Qi, N. T. Jafferis, K. LyonsJr., C. M. Lee, H. Ahmad, M. C. McAlpine, *Nano Lett.* **2010**, *10*, 524-528; b) Y. Qi, M. C. McAlpine, *Energy Environ. Sci.* **2010**, *3*, 1275-1285; c) D. J. Lipomi, Z. Bao, *Energy Environ. Sci.* **2011**, *4*, 3314-3328; d) F.-R. Fan, Z.-Q. Tian, Z. L. Wang, *Nano Energy* **2012**, *1*, 328-334.

[7] a) V. F. Curto, S. Coyle, R. Byrne, N. Angelov, D. Diamond, F. Benito-Lopez, *Sens. Actuators, B* **2012**, *175*, 263-270; b) J. Songok, M. Toivakka, *Microfluid. Nanofluid.* **2016**, *20*, 63; c) J. Songok, M. Toivakka, *ACS Appl. Mater. Interfaces* **2016**, *8*, 30523-30530.

[8] a) C. Chang, V. H. Tran, J. Wang, Y.-K. Fuh, L. Lin, *Nano Lett.* **2010**, *10*, 726-731; b) L. Dhakar, S. Gudla, X. Shan, Z. Wang, F. E. H. Tay, C.-H. Heng, C. Lee, *Sci. Rep.* **2016**, *6*, 22253; c) Y. Zi, H. Guo, Z. Wen, M.-H. Yeh, C. Hu, Z. L. Wang, *ACS Nano* **2016**, *10*, 4797-4805; d) P. Fan, Z.-h. Zheng, Y.-z. Li, Q.-y. Lin, J.-t. Luo, G.-x. Liang, X.-m. Cai, D.-p. Zhang, F. Ye, *Appl. Phys. Lett.* **2015**, *106*, 073901.

[9] M. Ma, Z. Kang, Q. Liao, Q. Zhang, F. Gao, X. Zhao, Z. Zhang, Y. Zhang, *Nano Res.* **2018**, DOI: 10.1007/s12274-12018-11997-12279.

[10] a) S. R. Anton, H. A. Sodano, *Smart Mater. Struct.* **2007**, *16*, R1; b) Z. L. Wang, G. Zhu, Y. Yang, S. Wang, C. Pan, *Mater. Today* **2012**, *15*, 532-543; c) J. Briscoe, S. Dunn, *Nano Energy* **2015**, *14*, 15-29.

[11] a) Z. L. Wang, *Sci. Am.* **2008**, *298*, 82-87; b) Z. L. Wang, *ACS Nano* **2013**, *7*, 9533-9557; c) X.-S. Zhang, M. Han, B. Kim, J.-F. Bao, J. Brugger, H. Zhang, *Nano Energy* **2018**, *47*, 410-426.

[12] a) K. Asif, A. Zafar, K. Heung Soo, O. Il-Kwon, *Smart Mater. Struct.* **2016**, *25*, 053002; b) T.-P. Huynh, H. Haick, *Adv. Mater.* **2016**, *28*, 138-143.

[13] B. Saravanakumar, S. Soyoon, S.-J. Kim, *ACS Appl. Mater. Interfaces* **2014**, *6*, 13716-13723.

[14] S. Garain, T. K. Sinha, P. Adhikary, K. Henkel, S. Sen, S. Ram, C. Sinha, D. Schmeißer, D. Mandal, *ACS Appl. Mater. Interfaces* **2015**, *7*, 1298-1307.

[15] M.-S. Noh, S. Kim, D.-K. Hwang, C.-Y. Kang, *Sens. Actuators, A* **2017**, *261*, 288-294.

[16] a) G. Zhu, W. Q. Yang, T. Zhang, Q. Jing, J. Chen, Y. S. Zhou, P. Bai, Z. L. Wang, *Nano Lett.* **2014**, *14*, 3208-3213; b) P. Bai, G. Zhu, Q. Jing, J. Yang, J. Chen, Y. Su, J. Ma, G. Zhang, Z. L. Wang, *Adv. Funct. Mater.* **2014**, *24*, 5807-5813.

[17] W. Xu, L. B. Huang, M. C. Wong, L. Chen, G. Bai, J. Hao, *Advanced Energy Materials* **2017**, *7*, 1601529.

[18] B.-U. Hwang, J.-H. Lee, T. Q. Trung, E. Roh, D.-I. Kim, S.-W. Kim, N.-E. Lee, *ACS Nano* **2015**, *9*, 8801-8810.

[19] S. Kim, M. K. Gupta, K. Y. Lee, A. Sohn, T. Y. Kim, K. S. Shin, D. Kim, S. K. Kim, K. H. Lee, H. J. Shin, D. W. Kim, S. W. Kim, *Adv. Mater.* **2014**, *26*, 3918-3925.

[20] J. Yang, P. Liu, X. Wei, W. Luo, J. Yang, H. Jiang, D. Wei, R. Shi, H. Shi, *ACS Applied Materials & Interfaces* **2017**, *9*, 36017-36025.

[21] X. Pu, L. Li, H. Song, C. Du, Z. Zhao, C. Jiang, G. Cao, W. Hu, Z. L. Wang, *Adv. Mater.* **2015**, *27*, 2472-2478.

[22] R. Zhang, S. Wang, M. H. Yeh, C. Pan, L. Lin, R. Yu, Y. Zhang, L. Zheng, Z. Jiao, Z. L. Wang, *Adv. Mater.* **2015**, *27*, 6482-6487.

[23] a) A. W. Van Herwaarden, P. M. Sarro, *SEns. Actuators* **1986**, *10*, 321-346; b) K. Uchida, S. Takahashi, K. Harii, J. Ieda, W. Koshibae, K. Ando, S. Maekawa, E. Saitoh, *Nature* **2008**, *455*, 778.
[24] a) A. Bulusu, D. G. Walker, *Superlattices Microstruct.* **2008**, *44*, 1-36; b) H. Alam, S. Ramakrishna, *Nano Energy* **2013**, *2*, 190-212; c) S. Twaha, J. Zhu, Y. Yan, B. Li, *Renewable Sustainable Energy Rev.* **2016**, *65*, 698-726; d) B. Iezzi, K. Ankireddy, J. Twiddy, M. D. Losego, J. S. Jur, *Appl. Energy* **2017**, *208*, 758-765.
[25] L. Francioso, C. D. Pascali, I. Farella, C. Martucci, P. Cretì, P. Siciliano, A. Perrone, *J. Power Sources* **2011**, *196*, 3239-3243.
[26] F. Zhang, Y. Zang, D. Huang, C.-a. Di, D. Zhu, *Nat. Commun.* **2015**, *6*, 8356.
[27] a) S. Günes, H. Neugebauer, N. S. Sariciftci, *Chem. Rev.* **2007**, *107*, 1324-1338; b) M. Pagliaro, R. Ciriminna, G. Palmisano, *ChemSusChem* **2008**, *1*, 880-891; c) M. Toivola, J. Halme, K. Miettunen, K. Aitola, P. D. Lund, *Int. J. Energy Res.* **2009**, *33*; d) G. Li, R. Zhu, Y. Yang, *Nat. Photonics* **2012**, *6*, 153-161; e) M. Kaltenbrunner, M. S. White, E. D. Głowacki, T. Sekitani, T. Someya, N. S. Sariciftci, S. Bauer, *Nature Communications* **2012**, *3*, 770.
[28] W. Y. Toh, Y. K. Tan, W. S. Koh, L. Siek, *IEEE Sens. J.* **2014**, *14*, 2299-2306.
[29] M. Magno, G. A. Salvatore, S. Mutter, W. Farrukh, G. Troester, L. Benini, in *IEEE International Symposium on Circuits and Systems (ISCAS)*, Montreal, QC, **2016**, pp. 337-340.
[30] J. Heikenfeld, *IEEE Spectr.* **2014**, *51*, 46-63.
[31] S. Lemey, S. Agneessens, P. V. Torre, K. Baes, J. Vanfleteren, H. Rogier, *IEEE Trans. Microwave Theory Tech.* **2016**, *64*, 2304-2314.
[32] a) R. Singh, E. Singh, H. S. Nalwa, *RSC Adv.* **2017**, *7*, 48597-48630; b) F. K. Shaikh, S. Zeadally, *Renewable Sustainable Energy Rev.* **2016**, *55*, 1041-1054.
[33] P. Kassal, M. D. Steinberg, I. M. Steinberg, *Sens. Actuators, B* **2018**, *266*, 228-245.
[34] J. Yoo, L. Yan, S. Lee, Y. Kim, H.-J. Yoo, *IEEE J. Solid-State Circuits* **2010**, *45*, 178-188.
[35] D. Shuaib, L. Ukkonen, J. Virkki, S. Merilampi, in *2017 IEEE 5th International Conference on Serious Games and Applications for Health (SeGAH)*, **2017**, pp. 1-5.
[36] J. Jun, J. Oh, D. H. Shin, S. G. Kim, J. S. Lee, W. Kim, J. Jang, *ACS Appl. Mater. Interfaces* **2016**, *8*, 33139-33147.
[37] J. S. Lee, J. Oh, J. Jun, J. Jang, *ACS Nano* **2015**, *9*, 7783-7790.
[38] K. Hu, R. Xiong, H. Guo, R. Ma, S. Zhang, Z. L. Wang, V. V. Tsukruk, *Adv. Mater.* **2016**, *28*, 3549-3556.
[39] a) A. Koh, D. Kang, Y. Xue, S. Lee, R. M. Pielak, J. Kim, T. Hwang, S. Min, A. Banks, P. Bastien, M. C. Manco, L. Wang, K. R. Ammann, K.-I. Jang, P. Won, S. Han, R. Ghaffari, U. Paik, M. J. Slepian, G. Balooch, Y. Huang, J. A. Rogers, *Sci. Transl. Med.* **2016**, *8*, 366ra165; b) A. Hitoshi, K. Jeonghyun, Z. Shaoning, B. Anthony, C. K. E., S. Xing, G. Philipp, S. Yunzhou, P. R. M., R. J. A., *Adv. Funct. Mate.* **2017**, *27*, 1604465; c) K. S. Bong, Z. Yi, W. S. Min, B. A. J., S. Yurina, X. Yeguang, K. Jahyun, H. S. W., M. J. A., P. J. Min, R. T. R., C. K. E., L. Kyu‐Tae, C. Jungil, P. R. L., G. C. C., S. A. J., C. Yu‐Yu, X. Shuai, K. Jeonghyun, K. Ahyeon, H. J. Sook, H. Yonggang, K. S. Wook, R. J. A., *Small* **2018**, *14*, 1703334.
[40] K. K. Ng, M. Takada, C. C. S. Jin, G. Zheng, *Bioconjugate Chem.* **2015**, *26*, 345-351.
[41] a) H. Irschik, *Eng. Struct.* **2002**, *24*, 5-11; b) K. Kruusamäe, A. Punning, A. Aabloo, K. Asaka, *Actuators* **2015**, *4*, 17-38.
[42] C. Rendl, H. M., I. S., K. D., F. S., P. P., R. C., T. J., Z. M., S. G., T. Rothländer, in *the 27th annual ACM symposium*, Honolulu, Hawaii, USA, **2014**, pp. 129–138.
[43] a) X. Lee, T. Yang, X. Li, R. Zhang, M. Zhu, H. Zhang, D. Xie, J. Wei, M. Zhong, K. Wang, D. Wu, Z. Li, H. Zhu, *Appl. Phys. Lett.* **2013**, *102*, 163117; b) R. Jan, A. Habib, Z. M. Khan, M. B. Khan, M. Anas, A. Nasir, S. Nauman, *J. Intell. Mater. Syst. Struct.* **2016**, 1-10; c) M. Ramirez, D. D. L. Chung, *Carbon* **2016**, *110*, 8-16; d) S. Nag-Chowdhury, H. Bellegou, I. Pillin, M. Castro, P. Longrais, J. F.

Feller, *Compos. Sci. Technol.* **2016**, *123*, 286-294; e) X. Xu, H. Li, Q. Zhang, H. Hu, Z. Zhao, J. Li, J. Li, Y. Qiao, Y. Gogotsi, *ACS Nano* **2015**, *9*, 3969-3977; f) E. Koch, A. Dietzel, *Sens. Actuators, A* **2016**, *250*, 138-144; g) E. Koch, A. Dietzel, *Sens. Actuators, A* **2017**, *267*, 293-300.

[44] a) R. P. Wool, *Soft Matter* **2008**, *4*, 400-418; b) B. J. Blaiszik, S. L. B. Kramer, S. C. Olugebefola, J. S. Moore, N. R. Sottos, S. R. White, *Annu. Rev. Mater. Res.* **2010**, *40*, 179-211; c) K. V. Tittelboom, N. D. Belie, *Materials* **2013**, *6*, 2182-2217.

[45] N. Roy, B. Bruchmann, J. M. Lehn, *Chem. Soc. Rev.* **2015**, *44*, 3786-3807.

[46] a) S. R. White, N. R. Sottos, P. H. Geubelle, J. S. Moore, M. R. Kessler, S. R. Sriram, E. N. Brown, S. Viswanathan, *Nature* **2001**, *409*, 794-797; b) M. R. Kessler, N. R. Sottos, S. R. White, *Composites: Part A* **2003**, *34*, 743-753; c) E. N. Brown, M. R. Kessler, N. R. Sottos, S. R. White, *J. Microencapsulation* **2003**, *20*, 719-730.

[47] a) S. Burattini, B. W. Greenland, D. Chappell, H. M. Colquhoun, W. Hayes, *Chem. Soc. Rev.* **2010**, *39*, 1973-1985; b) M. Le Neindre, R. Nicolay, *Polym. Chem.* **2014**, *5*, 4601-4611; c) P. Cordier, F. Tournilhac, C. Soulie-Ziakovic, L. Leibler, *Nature* **2008**, *451*, 977-980.

[48] a) D.-H. Kim, R. Ghaffari, N. Lu, J. A. Rogers, *Annu. Rev. Biomed. Eng.* **2012**, *14*, 113-128; b) J. Li, L. Geng, G. Wang, H. Chu, H. Wei, *Chem. Mater.* **2017**, *29*, 8932-8952.

[49] T.-P. Huynh, P. Sonar, H. Haick, *Adv. Mater.* **2017**, *29*, 1604973.

[50] B. C. K. Tee, C. Wang, R. Allen, Z. Bao, *Nature Nanotechnol.* **2012**, *7*, 825-832.

[51] K. Guo, D.-L. Zhang, X.-M. Zhang, J. Zhang, L.-S. Ding, B.-J. Li, S. Zhang, *Angew. Chem. Int. Ed.* **2015**, *54*, 12127-12133.

[52] E. D'Elia, S. Barg, N. Ni, V. G. Rocha, E. Saiz, *Adv. Mater.* **2015**, *27*, 4788-4794.

[53] P. R. Bandaru, *J. Nanosci. Nanotechnol.* **2007**, *7*, 1-29.

[54] a) P. M. Ajayan, L. S. Schadler, C. Giannaris, A. Rubio, *Adv. Mater.* **2000**, *12*, 750-753; b) Z. Spitalsky, D. Tasis, K. Papagelis, C. Galiotis, *Prog. Polym. Sci.* **2010**, *35*, 357-401.

[55] J. K. W. Sandler, J. E. Kirk, I. A. Kinloch, M. S. P. Shaffer, A. H. Windle, *Polymer* **2003**, *44*, 5893-5899.

[56] M. Liao, P. Wan, J. Wen, M. Gong, X. Wu, Y. Wang, R. Shi, L. Zhang, *Adv. Funct. Mater.* **2017**, *27*.

[57] Z. Liu, S. J. Picken, N. A. M. Besseling, *Macromolecules* **2014**, *47*, 4531-4537.

[58] T. Wu, B. Chen, *J. Mater. Chem. C* **2016**, *4*, 4150-4154.

[59] H. Jin, T.-P. Huynh, H. Haick, *Nano Lett.* **2016**, *16*, 4194-4202.

[60] a) Y. Y. Broza, P. Mochalski, V. Ruzsanyi, A. Amann, H. Haick, *Angew. Chem. Int. Ed.* **2015**, *54*, 11036-11048; b) Y. Y. Broza, L. Zuri, H. Haick, *Sci. Rep.* **2014**, *4*, 4611.

[61] a) H. Sun, X. You, Y. Jiang, G. Guan, X. Fang, J. Deng, P. Chen, Y. Luo, H. Peng, *Angew. Chem. Int. Ed.* **2014**, *53*, 9526-9531; b) J. Cao, C. Lu, J. Zhuang, M. Liu, X. Zhang, Y. Yu, Q. Tao, *Angew. Chem. Int. Ed.* **2017**, *56*, 8795-8800.

[62] B. Zhang, P. Zhang, H. Zhang, C. Yan, Z. Zheng, B. Wu, Y. Yu, *Macromol. Rapid Commun.* **2017**, *38*, 1700110.

[63] L. Qu, L. Dai, M. Stone, Z. Xia, Z. L. Wang, *Science* **2008**, *322*, 238-242.

[64] C. D. Meyer, C. S. Joiner, J. F. Stoddart, *Chem. Soc. Rev.* **2007**, *36*, 1705-1723.

[65] A. J. Bandodkar, V. Mohan, C. S. López, J. Ramírez, J. Wang, *Adv. Electron. Mater.* **2015**, *1*, 1500289.

[66] a) S. A. Odom, S. Chayanupatkul, B. J. Blaiszik, O. Zhao, A. C. Jackson, P. V. Braun, N. R. Sottos, S. R. White, M. J. S., *Adv. Mater.* **2012**, *24*, 2578-2581; b) B. J. Blaiszik, S. L. B. Kramer, M. E. Grady, D. A. McIlroy, J. S. Moore, N. R. Sottos, S. R. White, *Adv. Mater.* **2012**, *24*, 398-401.

[67] D. Chen, D. Wang, Y. Yang, Q. Huang, S. Zhu, Z. Zheng, *Adv. Energy Mater.* **2017**, *7*, 1700890.

[68] a) K. Parida, V. Kumar, W. Jiangxin, V. Bhavanasi, R. Bendi, P. S. Lee, *Adv. Mater.* **2017**, *29*, 1702181; b) W. Xu, L.-B. Huang, J. Hao, *Nano Energy* **2017**, *40*, 399-407.

[69] H. Zheng, Y. Zi, X. He, H. Guo, Y.-C. Lai, J. Wang, S. L. Zhang, C. Wu, G. Cheng, Z. L. Wang, *ACS Appl. Mater. Interfaces* **2018**, *10*, 14708-14715.

[70] a) Y. Zhan, Y. Mei, L. Zheng, *J. Mater. Chem. C* **2014**, *2*, 1220-1232; b) S. M. R. Islam, D. Kwak, M. H. Kabir, M. Hossain, K. S. Kwak, *IEEE Access* **2015**, *3*, 678-708; c) J. Wang, W. Ding, L. Pan, C. Wu, H. Yu, L. Yang, R. Liao, Z. L. Wang, *ACS Nano* **2018**, *12*, 3954-3963.

[71] B. Robert, *Sens. Rev.* **2014**, *34*, 137-142.

[72] TELECOMMUNICATION STANDARDIZATION SECTOR OF ITU, Geneva, Switzerland, **2012**, pp. Recommendation ITU-T Y.2060.

[73] W. Su, Z. Wu, Y. Fang, R. Bahr, P. M. Raj, R. Tummala, M. M. Tentzeris, in *IEEE MTT-S International Microwave Symposium (IMS)*, IEEE, Honololu, HI, USA, **2017**, pp. 544-547.

[74] a) C. H. Yang, C. C. Su, K. P. Hsieh, Y. R. Li, K. Y. Yeh, S. H. Chang, in *19th International Conference on Solid-State Sensors, Actuators and Microsystems (TRANSDUCERS)*, IEEE, Kaohsiung, Taiwan, **2017**, pp. 1360-1363; b) G. A. Salvatore, J. Sülzle, F. D. Valle, G. Cantarella, F. Robotti, P. Jokic, S. Knobelspies, A. Daus, L. Büthe, L. Petti, N. Kirchgessner, R. Hopf, M. Magno, G. Tröster, *Adv. Funct. Mater.* **2017**, *27*, 1702390.

[75] https://www.plasticsportal.net/wa/plasticsEU~en_GB/function/conversions:/publish/common/upload/biodegradable_plastics/Ecoflex_F_Blend_C1200.pdf.